



Electromigration reliability of Sn–3.0Ag–0.5Cu/Cu–Zn solder joints

Jae-Yong Park¹ · Taeyoung Lee^{1,2} · Wonil Seo^{1,2} · Sehoon Yoo² · Young-Ho Kim¹

Received: 1 November 2018 / Accepted: 6 March 2019 / Published online: 11 March 2019
© Springer Science+Business Media, LLC, part of Springer Nature 2019

Abstract

The electromigration reliability and failure modes of Sn–3.0Ag–0.5Cu (SAC)/Cu–Zn solder joints were investigated at 146 °C and a current density of 1.1×10^4 A/cm². After aging at 146 °C for 150 h without electric current, typical bi-layers of Cu₆Sn₅ and Cu₃Sn intermetallic compounds (IMCs) were formed in the SAC/Cu joints, whereas a single Cu₆(Sn, Zn)₅ phase was observed in the SAC/Cu–Zn joint. The total thickness of the IMC layer in the SAC/Cu–Zn specimen was thinner than that in the SAC/Cu specimen. After current stressing for 150 h on the anode side, the total thickness of the IMC layers of both types of solder joints was thicker than that without electric current. On the cathode side, the IMCs, Cu₆Sn₅ of SAC/Cu and Cu₆(Sn, Zn)₅ of SAC/Cu–Zn joints dissolved, and voids induced by electromigration propagated along the solder/IMC interfaces. Suppressed void formation was observed at the SAC/Cu–Zn interface when compared to the SAC/Cu interface. Further, electric current was applied to the solder joints until failure and the electromigration lifetime was plotted as a function of the Weibull cumulative distribution to examine the electromigration reliability of the solder joints. The mean time-to-failure of the SAC/Cu–Zn joint was two times longer than that of the SAC/Cu joint. Owing to the anisotropic behavior of Sn, two failure modes, the dissolution of the Cu pad (mode 1) and void propagation at the solder/IMC interface (mode 2) were observed in the SAC/Cu and SAC/Cu–Zn joints. In both specimens, the failure time of mode 2 was longer than that of mode 1. However, the main failure type was mode 1 in SAC/Cu joints and mode 2 in SAC/Cu–Zn joints. For both failure modes, the lifetime of Cu–Zn specimens was longer than that of Cu specimens. The electromigration reliability of the SAC/Cu–Zn joint was found to be superior to that of the SAC/Cu joint because the occurrence of failure mode 1 was suppressed and the lifetime of the SAC/Cu joint in both failure modes was longer.

1 Introduction

Cu–Zn wetting layers are being developed as Pb-free solders to replace Cu wetting layers [1–3]. In the case of Sn–3.0Ag–0.5Cu (SAC 305)/Cu–Zn joints, a rapid growth of intermetallic compounds (IMCs) has been noted; further, the formation of large Ag₃Sn plates is suppressed in SAC/Cu joints [4, 5]. In addition, no microvoids or rough interfaces are observed between Cu₆Sn₅ and Cu–Zn layers in SAC/Cu–Zn joints [6]. These microstructural changes caused by the addition of Zn in the Cu layer enhance the reliability of solder joints [7, 8]. To use Cu–Zn alloys in the microelectronic packaging industry, eco-friendly Cu–Zn wetting layers

were successfully electroplated in a non-cyanide solution [9] and the wetting characteristics of the Cu–Zn layer with SAC 305 were found to be similar to those of a Cu layer [10]. Therefore, Cu–Zn alloys have attracted much attention as promising and highly reliable wetting layers for Pb-free solders.

Electromigration-induced failure is an important reliability issue for Pb-free solder joint. Electromigration refers to the mass transport of atomic flux caused by the momentum transfer of moving electrons in response to an electric field. As a decrease in the pitch size of solder bumps is inevitable in electronic devices, the current density in a solder bump has continuously increased [11]. When the diameter of a solder bump is below 50 μm, electromigration can induce the void formation and propagation at the solder interface, resulting in an open circuit failure of the solder joints [12]. In addition, current crowding effect induced in the solder joints owing to their unique geometries accelerates electromigration failure on the cathode side [13, 14]. Although many electromigration studies have focused on SAC/Cu

✉ Young-Ho Kim
kimyh@hanyang.ac.kr

¹ Division of Materials Science & Engineering, Hanyang University, Seoul 133-791, South Korea

² Welding and Joining R&D Group, Korea Institute of Industrial Technology, Incheon 406-840, South Korea

joints, the electromigration behavior of SAC/Cu–Zn joints has not been reported thus far.

In this study, the electromigration reliabilities and failure modes of SAC/Cu–Zn joints were investigated to test the potential of Cu–Zn alloys as reliable wetting layers for Pb-free solders. The Cu–Zn alloy was electroplated in a non-cyanide solution at neutral pH to prevent damage to the polymer materials. SAC/Cu joints were also fabricated to compare the electromigration reliability with SAC/Cu–Zn joints. After current stressing, the failure times and modes of both solder joints were analyzed to understand their failure mechanisms under electromigration.

2 Materials and methods

Test specimens were fabricated by connecting two substrates, as shown schematically in Fig. 1. To fabricate the specimens and measure electrical resistance in a simple manner, a test specimen was designed to create an electrical path using two solder balls [15]. Printed circuit boards

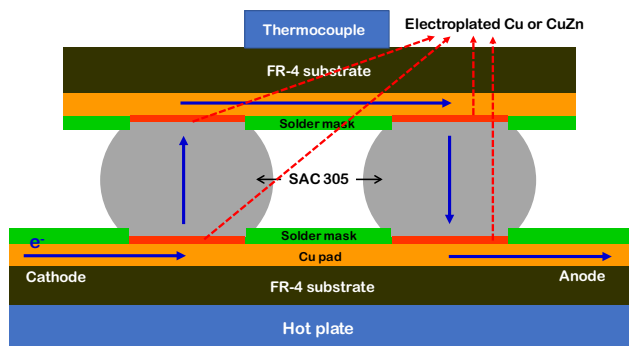


Fig. 1 A schematic illustrating electromigration testing of solder joints

(PCBs) composed of high T_g flame-resist 4 (FR-4) were used as the substrates. The thickness and opening size of the Cu pad on the PCB substrate were 35 and 220 μm , respectively. A Cu-20 wt% Zn layer was electroplated on the Cu pad of the PCB substrate. The electroplating bath of the Cu–Zn alloy consisted of a pyrophosphate-based solution at pH 7.8. For comparison, a Cu layer was electroplated on the substrate using a solution of copper sulfate and sulfuric acid [16]. The thickness of the electroplated Cu and Cu–Zn layers was 15 μm . Sn–3.0Ag–0.5Cu (SAC 305) solder balls with 300 μm diameter were used in this study. The solder balls were placed on Cu or Cu–Zn layers electroplated on the tops of PCBs after dispensing the water-soluble flux and reflowed at a peak temperature of 260 $^{\circ}\text{C}$ for 30 s. The top PCB with solder bumps was aligned with the bottom PCB and reflowed once more to fabricate electromigration specimens.

X-ray analysis (Xavis, XSCAN-H160-OCT) was carried out to observe void formation in the test specimens. Figure 2a shows the top-view X-ray images of the solder joints of the test specimens. Electric current was passed through the two solder balls located in the center of the test specimen. Figure 2b, c show magnified images of the solder joints located in the center of each specimen featuring large voids. A large void was a void with an area larger than 10% of the solder joint area. Specimens containing large voids in the solder joints were not used for electromigration tests.

Electromigration tests were conducted on a hotplate heated to 146 $^{\circ}\text{C}$. Because current densities of 10^4 – 10^5 A/ cm^2 can induce void formation and early failure [12], the electric current passing through the solder joints was maintained constant at 4.18 A (GW Instek, PSM-2010), corresponding to a current density of 1.1×10^4 A/ cm^2 . The temperature was monitored by attaching a thermocouple to the surface of the top substrate. The temperatures measured at the top substrate with or without current stressing were 150 and 134 $^{\circ}\text{C}$, respectively. Joule heating induced by the

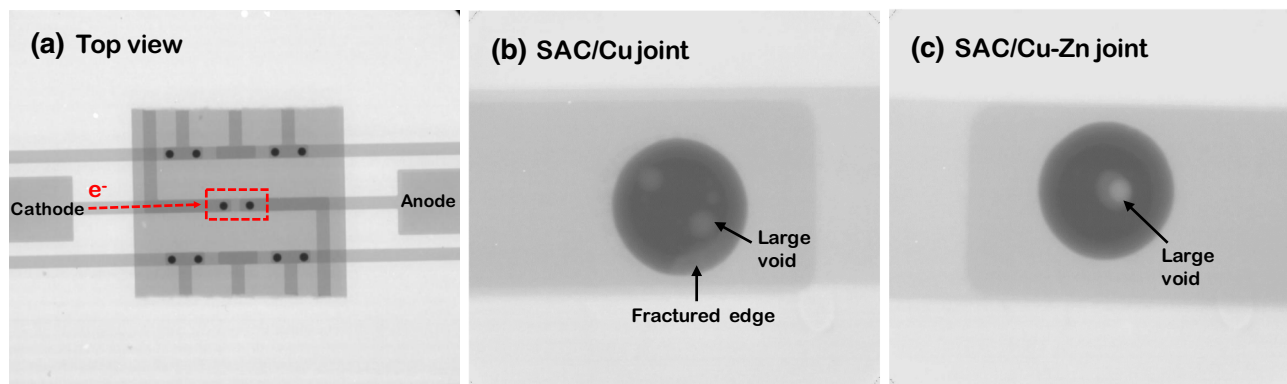


Fig. 2 X-ray images showing large voids in the solder joints. **a** Top view of the test specimen. Magnified images of the **b** SAC/Cu joint and **c** SAC/Cu–Zn joint

electric current led to an increase in the temperature of the surface of the top substrate by 16 °C. Firstly, the test specimens of SAC/Cu and SAC/Cu–Zn joints were aged for 150 h with or without passing electric current, and the evolution of the interfacial microstructure induced by electromigration was observed. A current density of 1.1×10^4 A/cm² was applied to ten specimens with either SAC/Cu or SAC/Cu–Zn joints to assess the lifetime of electromigration. The failure criterion for the electromigration tests was defined as a 20% increase in the resistance of the sample relative to the initial value [17]. The microstructures of the solder joints were characterized by scanning electron microscopy (SEM, JEOL, JSM-6300) before and after current stressing. The chemical composition of Cu–Zn IMC was analyzed by energy dispersive spectroscopy (EDS, AMETEK EDAX, Octane Elect Plus). Finally, the void formation and failure modes of the solder joints were analyzed to investigate the failure mechanism.

3 Results and discussion

3.1 Interfacial microstructures of solder joints aged for 150 h without electric current

Figure 3 shows the cross-sectional back-scattered electron (BSE) images of the as-fabricated solder joints before passing electric current. At the solder/Cu interfaces, a typical scallop-like Cu_6Sn_5 IMC was formed after reflowing.

To fabricate the SAC/Cu–Zn joint, a Cu–Zn layer was electroplated in a neutral solution. A $\text{Cu}_6(\text{Sn}, \text{Zn})_5$ IMC was observed at the SAC/Cu–Zn interface because small quantities of Zn atoms dissolved in the Cu_6Sn_5 phase during reflow. The Gibbs free energy of formation of $\text{Cu}_6(\text{Sn}, \text{Zn})_5$ was lower than that of the formation of Cu_6Sn_5 [18]. The initial thickness of the IMC layer of the Cu–Zn specimen was found to be slightly smaller than that of the Cu specimen, irrespective of the reflow numbers. In both specimens, the IMC layers of twice-reflowed regions were slightly thicker than those of once-reflowed regions. The interfacial microstructures of SAC/Cu and SAC/Cu–Zn joints aged at 146 °C (hot plate temperature) for 150 h without passing electric current are presented in Fig. 4. After aging, the IMC layer at the solder interfaces thickened and flattened in both Cu and Cu–Zn specimens. Cu_3Sn and microvoids formed at the $\text{Cu}_6\text{Sn}_5/\text{Cu}$ interfaces, while only $\text{Cu}_6(\text{Sn}, \text{Zn})_5$ grew at the solder/Cu–Zn interfaces. Further, Cu–Zn IMCs were not observed at the $\text{Cu}_6(\text{Sn}, \text{Zn})_5/\text{Cu–Zn}$ interfaces. The total IMC thickness of the SAC/Cu–Zn joints was thinner than that of SAC/Cu joints because the Zn accumulation layer at the $\text{Cu}_6(\text{Sn}, \text{Zn})_5/\text{Cu–Zn}$ interface hindered the diffusion of Sn and Cu atoms [4]. All the results obtained this study were similar to those of our previous study, wherein Cu–Zn layers were electroplated in an alkaline solution [9]. The formation and growth of Cu_3Sn and microvoids has been described in detail elsewhere [19].

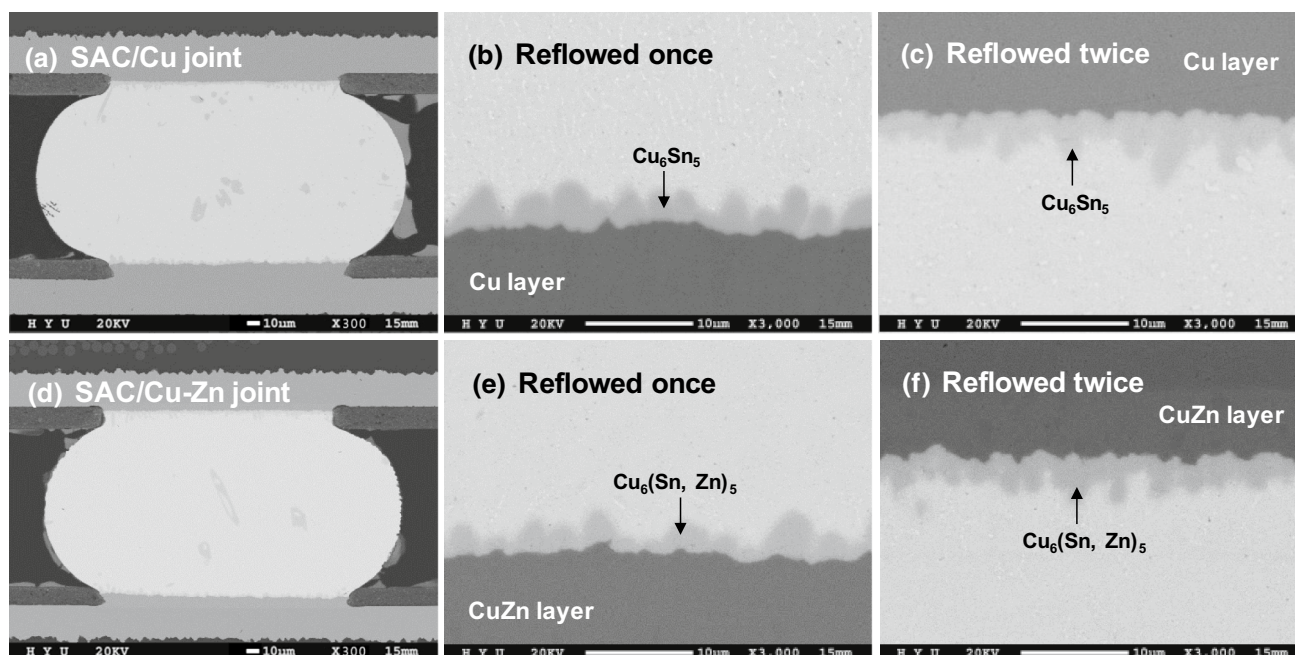
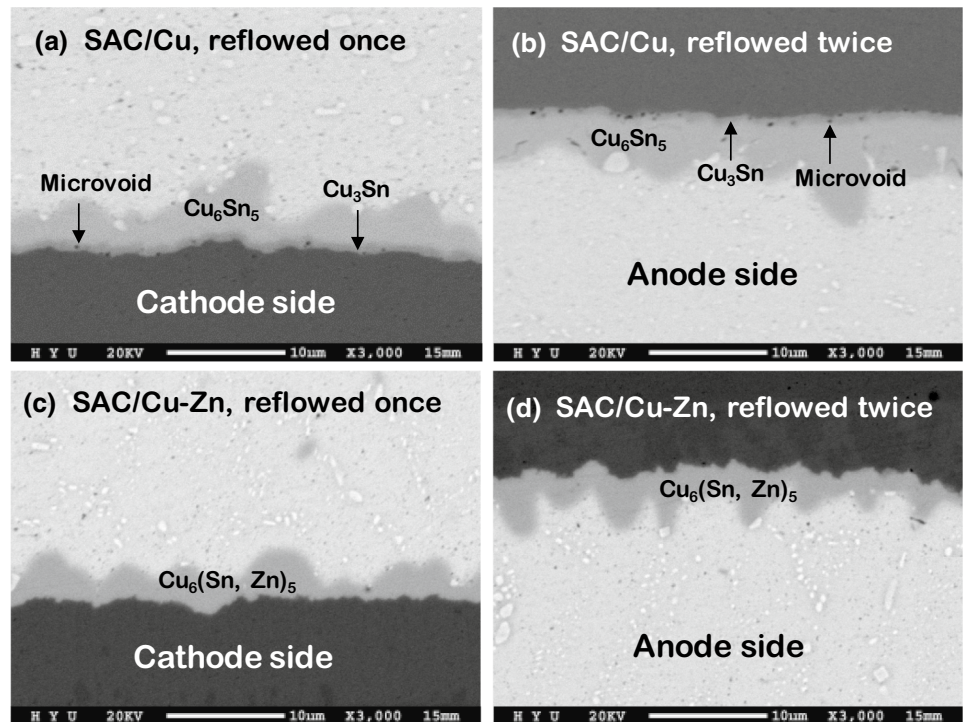


Fig. 3 Cross-sectional BSE images of solder joints without electric current. **a** SAC/Cu joint, **b** SAC/Cu joint reflowed once, **c** SAC/Cu joint reflowed twice, **d** SAC/Cu–Zn joint, **e** SAC/Cu–Zn joint reflowed once, and **f** SAC/Cu–Zn joint reflowed twice

Fig. 4 Interfacial microstructures of the solder joints after aging at 146 °C for 150 h without current stressing: **a, b** SAC/Cu joints; **c, d** SAC/Cu–Zn joints

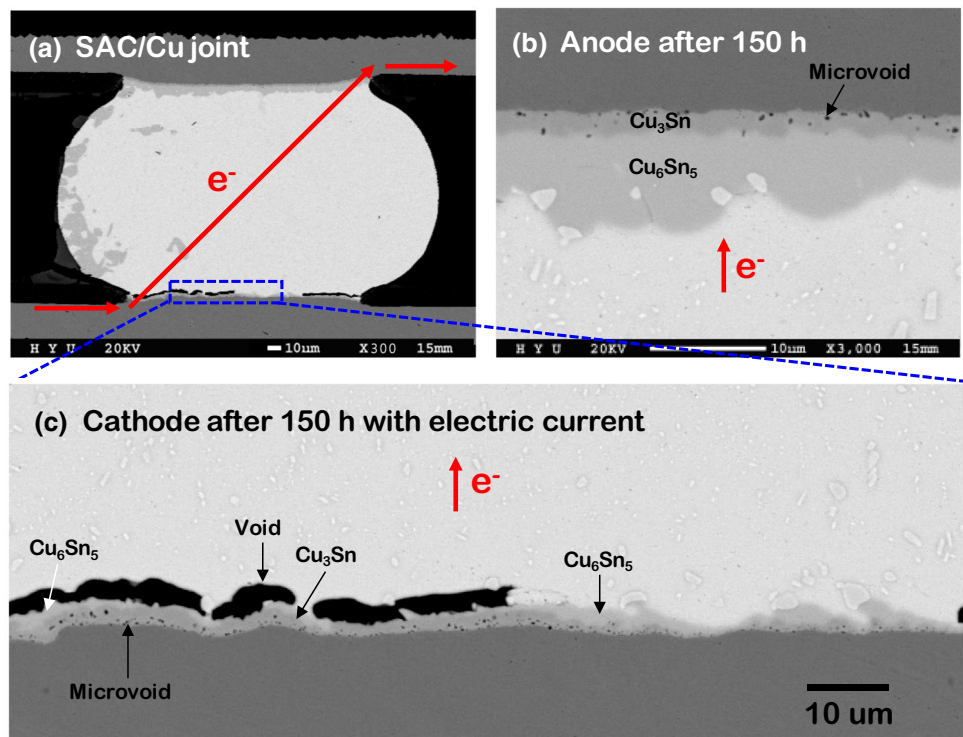


3.2 Interfacial microstructure after aging the joints for 150 h at a current density of 1.1×10^4 A/cm²

Figure 5 shows the cross-sectional BSE images of SAC/Cu joints aged at 146 °C for 150 h at a current density of

1.1×10^4 A/cm². On the anode side, the Cu₆Sn₅ IMC rapidly grew and a Cu₃Sn IMC with micro-voids was observed beneath Cu₆Sn₅. The morphology of Cu₆Sn₅ changed to a layered type [20]. In contrast, on the cathode side, voids induced by electromigration were observed, while the

Fig. 5 Cross-sectional BSE images of a SAC/Cu joint after current stressing for 150 h. **a** SAC/Cu joint, **b** anode side, and **c** cathode side



thickness of Cu_6Sn_5 IMC at the solder interface decreased significantly. Microvoids were formed in the Cu_3Sn layer by impurities in electroplated Cu and the large voids induced by electromigration were attributed to the self-diffusion of Sn in the solder [16, 21]. On the anode side, the number of microvoids formed with the passage of electric current was higher than the number of microvoids formed without electric current, thus indicating that the reaction between Sn and Cu was accelerated by current stressing. This result was consistent with that of a previous study [15]. Because the thickness of the Cu_6Sn_5 layer below the voids was thinner than that of Cu_6Sn_5 below the solder on the cathode side, IMC dissolution was attributed to void formation and propagation. Owing to the polarity of the electric current, the IMC layer on the anode side was thicker than that on the cathode side. The effect of polarity on IMC growth on the anode and cathode sides was found to be consistent with the results of a study by Gan and Tu [22].

Figure 6 is the BSE images showing the interfacial microstructure of a SAC/Cu–Zn joint aged at 146 °C for 150 h at a current density of $1.1 \times 10^4 \text{ A/cm}^2$. Only the $\text{Cu}_6(\text{Sn}, \text{Zn})_5$ IMC grew and flattened on the anode side. However, on the cathode side, a void induced by electromigration was observed at the solder/ $\text{Cu}_6(\text{Sn}, \text{Zn})_5$ interface and the Cu–Zn IMC formed inside the $\text{Cu}_6(\text{Sn}, \text{Zn})_5$ IMC. The chemical composition of Cu–Zn IMC was 51.6 at.% Cu, 39.8 at.% Zn, and 8.6 at.% Sn. Further, microvoids were not observed because Cu_3Sn was not formed. The $\text{Cu}_6(\text{Sn}, \text{Zn})_5$ layer was found to be thinner compared to that of the specimen not

subjected to current stressing, indicating that $\text{Cu}_6(\text{Sn}, \text{Zn})_5$ was dissolved by electromigration. Excessive IMC growth occurred on the anode side, while IMC dissolution occurred on the cathode side for both Cu and Cu–Zn specimens. To examine the effect of polarity on electromigration and IMC growth, IMC thickness on the anode side after aging the specimens at 146 °C for 150 h with or without current stressing was measured (Fig. 7). A precise comparison between IMC thicknesses with and without electromigration on the cathode side was difficult due to their dissolution. However, on the anode side, the following observations were

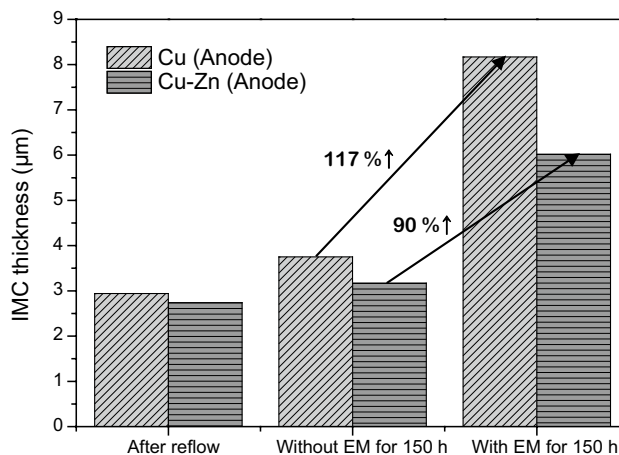
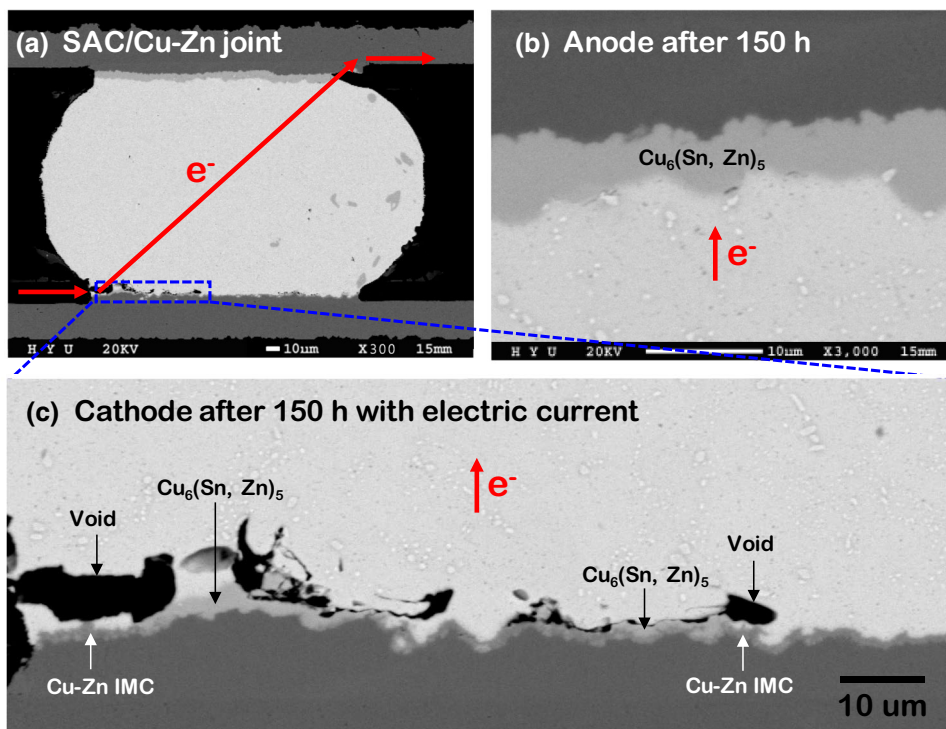


Fig. 7 Total IMC thickness on the anode side with or without current stressing (EM electromigration)

Fig. 6 Cross-sectional BSE images of a SAC/Cu–Zn joint after current stressing for 150 h. a SAC/Cu–Zn joint, b anode side, and c cathode side



made for both samples. (i) The total IMC thickness of joints aged without current stressing was increased than that after reflow; (ii) the overall IMC thickness after aging with electric current was increased than that without electric current; (iii) a thicker IMC layer was formed with electric current in the Cu specimen than in the Cu–Zn specimen. As a consequence of electromigration, the IMC thickness increased to 117% in the SAC/Cu joint and to 90% in the SAC/Cu–Zn joint.

3.3 Electromigration reliability and failure modes in solder joints

3.3.1 Electromigration reliability

To investigate the electromigration reliability of SAC/Cu and SAC/Cu–Zn joints, a current density of 1.1×10^4 A/cm² was applied until the solder joints failed. Figure 8 shows the Weibull cumulative distribution plots with respect to electromigration lifetime. The mean-time-to-failure (MTTF) was

found to be 459 h for the Cu specimen and 1176 h for the Cu–Zn specimen, indicating that the electromigration reliability of the Cu–Zn specimen was about two times higher than that of the Cu specimen. Figure 9 shows the two failure modes of the SAC/Cu joints after current stressing. Failure mode 1 involved Cu dissolution and failure mode 2 involved void propagation at the solder/IMC interface. The bulk solder was almost filled with IMC owing to Cu dissolution in failure mode 1, while void propagation along the solder/Cu₆Sn₅ interface resulted in open circuit failure in failure mode 2. Owing to the anisotropic behavior of Sn, two failure modes were observed in the solder joints after electromigration tests [21, 23]. On one hand, failure mode 1 occurred when the c-axis in the Sn grain was parallel to the direction of the electric current. As the diffusivity of Cu through the c-axis in the Sn grain was much faster than that through the a- or b-axes or the self-diffusion of Sn [24], Cu atoms rapidly diffused into the solder and reacted with Sn atoms, resulting in the dissolution of Cu and excessive growth of the IMC. On the other hand, failure mode 2 induced by

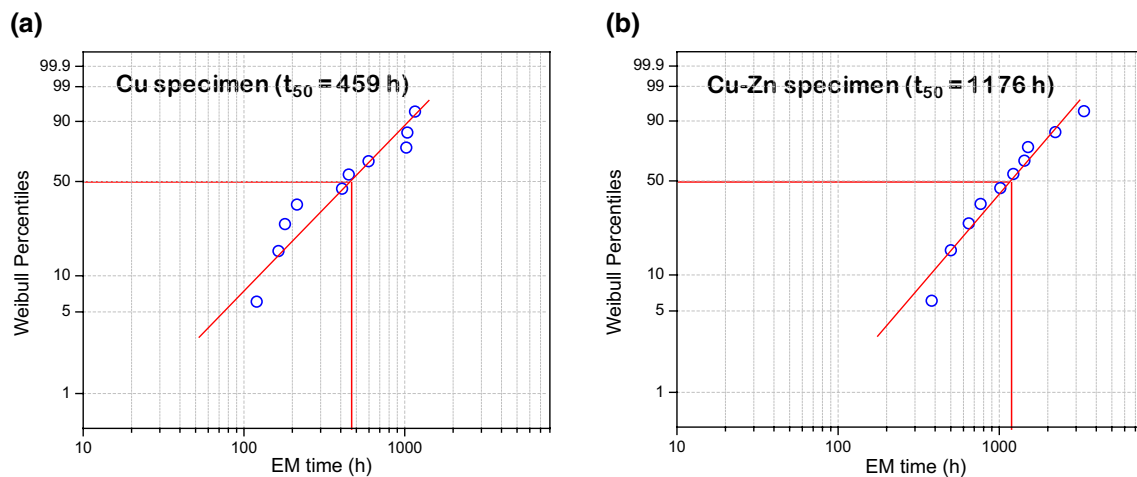


Fig. 8 Weibull cumulative distribution plots with respect to electromigration lifetime. **a** Cu specimens and **b** Cu–Zn specimens

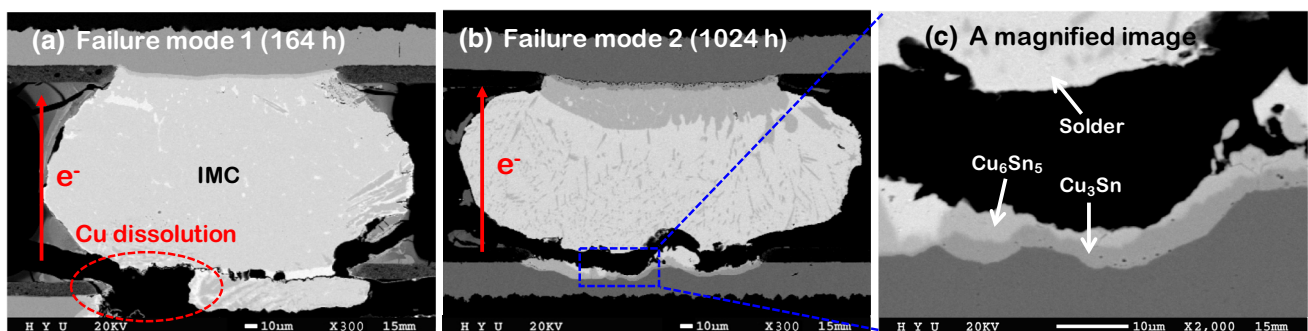


Fig. 9 Failure modes of SAC/Cu joints after the application of 1.1×10^4 A/cm² current density. **a** Failure mode 1 (164 h), **b** failure mode 2 (1024 h), and **c** a magnified image showing failure mode 2

void propagation was attributed to the self-diffusion of Sn when the direction of the electric current was along the a- or b-axes of the Sn grain. Under electromigration, atomic flux due to Sn self-diffusion induced vacancy accumulation on the cathode side. Furthermore, the vacancies condensed at the solder/IMC interface, resulting in void formation and propagation [22].

The two failure modes of the SAC/Cu–Zn joints after current stressing are presented in Fig. 10. Failure occurred due to Cu dissolution (failure mode 1) and void formation (failure mode 2) at the solder/IMC interface. The dissolved Cu filled the solder to form an IMC, and void propagation along the solder/Cu₆(Sn, Zn)₅ interface induced open circuit failure. In failure mode 2, the electroplated Cu–Zn layer was remained beneath the Cu–Zn IMC after electromigration tests. The rate of occurrence and average lifetime of the failure modes calculated from ten failed specimens after electromigration testing are listed in Table 1. Failure mode 1 was observed in eight specimens with SAC/Cu joints and in only four specimens with SAC/Cu–Zn joints, i.e., mode 1 was the major cause of failure in SAC/Cu joints, whereas mode 2 was the main cause of failure in SAC/Cu–Zn joints. The electromigration lifetime of failure mode 2 was longer than that of failure mode 1. In both failure modes, the average lifetimes of the Cu–Zn specimens were longer than those of Cu specimens.

During reflow soldering, small Zn atoms from the Cu–Zn layer dissolved in the SAC solder and modified the microstructure of the bulk solder as well as that of the solder/Cu–Zn interface. Because the Cu₆(Sn, Zn)₅ IMC grew in a random

orientation upon the addition of Zn to Cu₆Sn₅, the Sn grains adjacent to Cu₆(Sn, Zn)₅ became polycrystalline [25, 26]. Further, grain orientation was influenced by the orientation of adjacent grains during solidification [27]. As the randomly oriented grains of Sn suppressed fast Cu dissolution (failure mode 1) through their c-axis diffusion during current stressing, the occurrence of failure mode 1 was difficult in SAC/Cu–Zn joints. A similar result was obtained in a previous study comparing Zn-doped SnAg solders with SnAg solders [28]. Failure mode 1 caused early failure owing to the fast diffusion of Sn and Cu driven by current stressing, consequently resulting in a shorter lifetime for mode 1 when compared to failure mode 2. Thus, the electromigration reliability of SAC/Cu–Zn joints was improved by suppressing failure mode 1.

3.3.2 Comparison of the lifetimes of the failure modes

MTTF by electromigration was first proposed by J. R. Black using Al lines [29]. During current stressing, current crowding and Joule heating occurred due to the unique shape of the solder joint, resulting in a faster failure in shorter time periods when compared to the MTTF calculated from Black’s equation [11]. Black’s equation for MTTF by electromigration was modified to account for current crowding and Joule heating as follows [30]:

$$MTTF = A \frac{1}{(cj)^n} \exp \left[\frac{Q}{K(T + \Delta T)} \right]$$

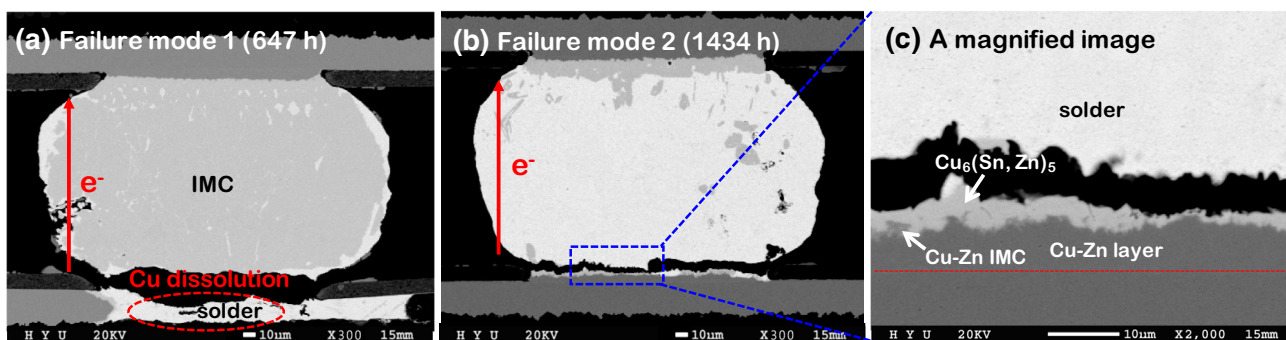


Fig. 10 Failure modes in SAC/Cu–Zn joints after the application of current at a density of 1.1×10^4 A/cm². **a** Failure mode 1 (647 h), **b** failure mode 2 (1434 h), and **c** a magnified image showing failure mode 2

Table 1 Rate of occurrence and average lifetimes of failure modes after electromigration tests

	SAC/Cu		SAC/Cu–Zn	
	Failure mode 1	Failure mode 2	Failure mode 1	Failure mode 2
Rate of occurrence (%)	80	20	40	60
Average lifetime (h)*	485	737	940	1551

*The average lifetime was calculated from failed specimens for each mode

where A is the constant cross-sectional area of the joint, c represents constant current crowding, j is the current density, n is a model parameter for the current density, Q is the activation energy, k is Boltzmann's constant, T is the average bump temperature, and ΔT is the increase in the temperature of the joint due to Joule heating. In the MTTF equation for the Cu and Cu–Zn specimens studied in this investigation, only the activation energies, Q , were different as the specimen structure and test conditions were identical. In failure mode 1, as the electromigration lifetime was equal to IMC growth time during which the Cu pad was entirely consumed [31], the activation energy for electromigration was similar to that of IMC growth [32]. The calculated activation energies for IMC growth in the SAC/Cu and SAC/Cu–Zn joints were 79.79 and 96.61 kJ/mol [4], respectively, indicating that the lifetime in mode 1 for the Cu–Zn specimen was longer.

With respect to failure mode 2, the SEM images in Figs. 9c and 10c clearly exhibit void propagation and open circuit failure at the solder/IMC interfaces. As failure mode 2 was attributed to Sn self-diffusion, microstructural changes occurring in the bulk solder after current stressing were important for analyzing electromigration reliability in SAC/Cu and SAC/Cu–Zn joints. Electron back-scattering diffraction studies [28] indicated lesser damage to the microstructure of the Zn-doped SnAg solder than that sustained by the SnAg solder after current stressing because no grain growth was observed and the Ag_3Sn and Cu_6Sn_5 IMC networks were stabilized in the Zn-doped SnAg solder. In other words, the addition of Zn to the solder enhanced electromigration reliability of solder joint. In our study, Zn atoms from the Cu–Zn layer also dissolved in the solder during reflow soldering. In addition, when the IMC layers on the anode side with and without electric current were compared, the IMC at the SAC/Cu interface was found to be thicker than that at the SAC/Cu–Zn interface, indicating that atomic diffusion through Sn by electromigration was more delayed in SAC/Cu–Zn joints. Therefore, the failure lifetime in mode 2 was longer in the Cu–Zn specimen than in the Cu specimens. As the rate of occurrence of failure mode 1 was suppressed and the failure lifetimes in modes 1 and 2 were longer for SAC/Cu–Zn joints, the electromigration reliability of SAC/Cu–Zn joints was significantly higher than that of SAC/Cu joints.

4 Conclusions

A current density of 1.1×10^4 A/cm² was applied to analyze the electromigration reliability and failure modes of SAC/Cu and SAC/Cu–Zn joints. After current stressing for 150 h, the total IMC thickness on the anode side was higher than that in specimens not subjected to current stressing. The IMC thickness increased to 117% in the SAC/Cu joint and

to 90% in the SAC/Cu–Zn joint owing to electromigration. On the cathode side, the IMCs were dissolved and voids were formed at the solder/IMC interface, indicating that polarity exerted a similar influence on IMC growth in both solder joints. Void formation induced by electromigration was suppressed at the SAC/Cu–Zn interface and the MTTF of the Cu–Zn specimen was found to be approximately twice as high as that of the Cu specimen. Two types of failure modes were observed in the solder joints. The failure mode 1 involved Cu dissolution indicating an early failure, and the failure mode 2 represented void propagation at the solder/IMC interface. The occurrence of mode 1 was suppressed in SAC/Cu–Zn joints due to the formation of polycrystalline grains at the solder interface. In addition, for both failure modes, the lifetimes of Cu–Zn specimens were longer than those of Cu specimens. Therefore, the SAC/Cu–Zn joints showed outstanding performance for electromigration reliability.

Acknowledgements This work was supported by the practical application project of the Multi-layered Composite Packaging Program (Grant Code #: 10041083) of the Korea Electronics-machinery Convergence Technology Institute, funded by the Ministry of Knowledge Economy.

References

1. C.-Y. Oh, H.-R. Roh, Y.M. Kim, J.S. Lee, H.Y. Cho, Y.-H. Kim, *J. Mater. Res.* **24**, 297–300 (2009)
2. C.-Y. Yu, J.-G. Duh, *J. Mater. Sci.* **47**, 6467–6474 (2012)
3. W.-Y. Chen, J.-G. Duh, *Mater. Lett.* **186**, 279–282 (2017)
4. Y.M. Kim, H.-R. Roh, S. Kim, Y.-H. Kim, *J. Electron. Mater.* **39**, 2504–2512 (2010)
5. Y.M. Kim, T.J. Kim, M.Y. Choi, Y.-H. Kim, *J. Alloys Compd.* **575**, 350–358 (2013)
6. Y.M. Kim, K.-M. Harr, Y.-H. Kim, *Electron. Mater. Lett.* **6**, 151–154 (2010)
7. J.-Y. Park, Y.M. Kim, Y.-H. Kim, *J. Mater. Sci.* **26**, 5852–5862 (2015)
8. C.-Y. Yu, W.-Y. Chen, J.-G. Duh, *J. Alloys Compd.* **586**, 633–638 (2014)
9. J.-Y. Park, Y.M. Kim, Y.-H. Kim, *J. Mater. Sci.* **27**, 5916–5924 (2016)
10. J.H. Lee, Y.M. Kim, J.H. Hwang, Y.-H. Kim, *J. Alloys Compd.* **567**, 10–14 (2013)
11. C. Chen, H.M. Tong, K.N. Tu, *Annu. Rev. Mater. Res.* **40**, 531–555 (2010)
12. Semiconductor Industry Association, *The International Technology Roadmap for Semiconductors*. (Semiconductor Industry Association, San Francisco, 2007)
13. E.C.C. Yeh, W.J. Choi, K.N. Tu, *Appl. Phys. Lett.* **80**, 580–582 (2002)
14. Y. Li, A.B.Y. Lim, K. Luo, Z. Chen, F. Wu, Y.C. Chan, *J. Alloys Compd.* **673**, 372–382 (2016)
15. Y. Jung, J. Yu, *J. Appl. Phys.* **115**, 083708 (2014)
16. J.-Y. Park, W. Seo, S. Yoo, Y.-H. Kim, *J. Alloys Compd.* **724**, 492–500 (2017)
17. J.M. Kim, M.-H. Jeong, S. Yoo, Y.-B. Park, *J. Electron. Mater.* **41**, 791–799 (2012)
18. C.-Y. Yu, J.-G. Duh, *Scr. Mater.* **65**, 783–786 (2011)

19. K. Zeng, R. Stierman, T.-C. Chiu, D. Edwards, K. Ano, K.N. Tu, *J. Appl. Phys.* **97**, 024508 (2005)
20. J. Feng, C. Hang, Y. Tian, C. Wang, B. Liu, *J. Alloys Compd.* **753**, 203–211 (2018)
21. M. Lu, D.-Y. Shih, P. Lauro, C. Goldsmith, D.W. Henderson, *Appl. Phys. Lett.* **92**, 211909 (2008)
22. H. Gan, K.N. Tu, *J. Appl. Phys.* **97**, 063514 (2005)
23. M. Sun, Z. Zhao, F. Hu, A. Hu, M. Li, H. Ling, T. Hang, *Electron. Mater. Lett.* **14**, 526–532 (2018)
24. T.L. Yang, J.J. Yu, C.C. Li, Y.F. Lin, C.R. Kao, *J. Alloys Compd.* **627**, 281–286 (2015)
25. C.-Y. Yu, W.-Y. Chen, J.-G. Duh, *Intermetallics* **26**, 11–17 (2012)
26. W.-Y. Chen, W. Tu, H.-C. Chang, T.-T. Chou, J.-G. Duh, *Mater. Lett.* **134**, 184–186 (2014)
27. J.O. Suh, K.N. Tu, N. Tamura, *Appl. Phys. Lett.* **91**, 051907 (2007)
28. M. Lu, D.-Y. Shih, S.K. Kang, C. Goldsmith, P. Flaitz, *J. Appl. Phys.* **106**, 053509 (2009)
29. J.R. Black, *IEEE Trans. Electron Devices* **16**, 338–347 (1969)
30. W.J. Choi, E.C.C. Yeh, K.N. Tu, *J. Appl. Phys.* **94**, 5665–5671 (2003)
31. M. Ding, Investigation of Electromigration Reliability of Solder Joint in Flip-Chip Packages, Ph. D. Dissertation, University of Texas at Austin, 2007
32. J.-H. Lee, Y.-B. Park, *J. Electron. Mater.* **38**, 2194–2200 (2009)

Publisher's Note Springer Nature remains neutral with regard to jurisdictional claims in published maps and institutional affiliations.